ACADEMIA ROMÂNĂ
Revue Roumaine de Chimie
https://www.icf.ro/rrch/

Rev. Roum. Chim.,
2022, *67*(4-5), 329–338
DOI: 10.33224/rrch.2022.67.4-5.12

PREPARATION OF HIGH QUALITY NICKEL OXIDE-COBALT OXIDE ELECTRODE MATERIALS ON CONDUCTIVE SUBSTRATES BY ELECTROCHEMICAL METHOD

Fatma BAYRAKÇEKEN NISANCI[a]

[a]Department of Chemistry, Faculty of Science, Ataturk University, 25240, Erzurum, Turkey

Received January 8, 2022

The main purpose of this paper is binary transition metal oxides NiO-Co_3O_4 which can provide high capacitance through alternating oxidation and reduction in wide potential range at low cost without any connector, flexible synthesis method, due to well-defined electrochemical behaviors and high theoretical capacity, provide better performance in batteries the future is to produce alternative electrode materials. Double metal oxide NiO-Co_3O_4 nanoparticles with high capacitance to show the electrodes were synthesized by a new electrochemical method in their application was investigated systematically. In this context, although many methods related to the synthesis of NiO-Co_3O_4 have been studied extensively, electrochemical methods with parameters that allow for more practical, environmentally friendly, inexpensive and inherently interfacial and size controlled material deposition have not yet been fully investigated. These compound semiconductors can be used at room temperature and atmospheric pressure, without additional steps and no further processing, NiO/Co_3O_4 nanostructured electrodes, again electrochemically synthesized, were prepared directly on ITO and the desired composition, structure, size, ITO/NiO/Co_3O_4 were readily synthesized by controlling the electrochemical parameters such as potential and time. The surface morphology of the prepared three dimensional (3D) electrodes, scanning electron microscopy (SEM), the chemical composition of energy dispersive X-ray spectroscopy (EDS) and X-ray photoelectron spectroscopy (XPS) characterization and the crystal structure analysis were made by X-ray diffraction XRD.

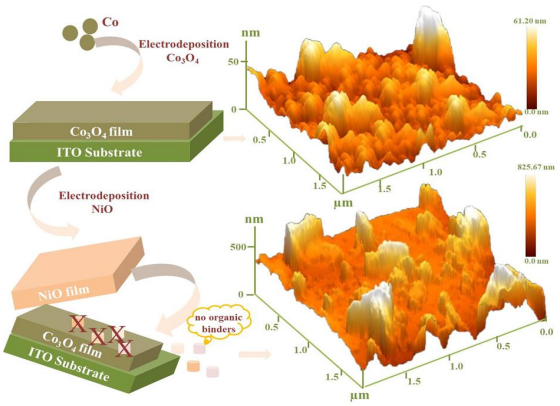

INTRODUCTION

One of the most challenging goals facing modern society is the capacity to make available at all times and conditions the increasing amount of energy produced from clean and renewable sources. It requires the use of inexpensive, efficient, and high-capacity rechargeable devices that must be integrated into smart energy distribution systems. For a wide range of applications, from portable devices to the current electric and hybrid vehicle model, lithium-ion batteries (LIBs) have met these requirements and are the leading technology for electrochemical energy recycling and energy storage.[1] In this context, different functional materials are continuously developing, and the structural properties and electrochemical properties of each are distinguished.[2] For all these reasons, there has recently been a strong interest in researching possible alternative solutions for LIBs, which covers a wide variety of applications ranging from consumer electronics (laptops, cell phones, and cameras, etc.) to electric vehicles (hybrid electric

* Corresponding author: fbayrakceken@atauni.edu.tr

cars and all-electric scooters). Comprehensive different researches are carried out to improve the features and eliminate the disadvantages of LIBs, which are defined as the technology of the future.

The synthesis, assembly, and application of Co_3O_4 (~2.4 eV band gap, high capacity semiconductor that can meet the requirements of storage and use of clean energy) nanostructures with different morphologies such as particles, tubes, wires, and rods have gained intense interest by Belcher et al.[3] In addition, NiO, with properties such as high surface-to-volume ratio and open edge geometry, represents an ideal two-dimensional (2D) structure and is used in battery materials, field emitters, and similar applications. With unique size and shape, NiO nanostructures can function at superior dimensions or open up new possibilities due to the large surface fraction and confinement effect inherent in reduced-size materials. In recent years, various types of NiO nanostructures have been synthesized, including nanowires, nanorods, nano sets, and nanospheres.[4] However, vertically oriented electrochemically synthesized NiO (~3.6 eV wide band gap antiferromagnetic semiconductor) nanostructures have not been fully elucidated yet. The performance of electrodes based on NiO-Co_3O_4 nanostructures is very good due to the unique properties of these nanoarrays, such as high surface areas, crystallinity, and direct growth on conductive substrates, and good conductivity. NiO-Co_3O_4 nanoarrays have higher specific capacities and better rate capabilities compared to their single components; When the charge-discharge rate is changed from 2 to 40 A/g, the capacitance for NiO-Co_3O_4 nanoarrays is maintained 85%, much higher than that of CoO nanowire arrays (76.7%) and NiO nanoflake arrays (66.6%).[5] In the research of Xia et al., the specific capacitance is 853 Fg^{-1} at a current density of 2 Ag^{-1} in electrodes coated with NiO nano pulse shells on Co_3O_4 nanowire.[6] Transition metal oxides such as NiO and Co_3O_4 are technologically important materials for electrodes used in LIBs. NiO and Co_3O_4 have been considered as the most promising electrode materials, characterized as low cost, more abundant, and environmentally friendly. However, disadvantages such as low electronic conductivity and capacitance value limited their applications. To meet these applications, it has been desirable to integrate these oxides into core-shell nanostructured arrays to achieve enhanced electrical, optical, electrochemical, and mechanical properties.[7] Therefore, new studies have been started to be combined with NiO and Co_3O_4 to overcome their disadvantages and take advantage of their advantages.[8] Compared to single metal oxides, NiO-Co_3O_4 binary transition metal oxide has attracted great attention due to its synergistic effect, and it has been stated that it contributes to its high conductivity, rich conversion stability, and high-speed performance.[9] Double layered nickel-cobalt is one of the promising electrode materials due to its high theoretical capacitance value >3000 F/g, a superior redox activity, and it is an economical as well as environmentally friendly chemical. There are several techniques that can be used to prepare metal oxides to be used as electrodes, such as sol-gel, chemical precipitation, hydrothermal preparation, chemical vapor deposition, and electrodeposition. In the case of sol-gel, co-precipitation, and hydrothermal preparation, the product produced is in powder form and needs a polymer binder to produce the electrode. This product increases resistance, clogs the pore space, and causes disintegration due to degradation over time. They are binding materials that can affect the power density of LIBs.[10] Therefore, the production of bondless thin electrodes constitutes a compelling strategy to reduce the internal resistance and maximize power density, as reported in previous studies.

Electrochemical production methods arouse great interest due to the unique principles and flexibility of electrode materials that control the structure and morphology of the electrode materials.[11,12] The main advantage of the electrochemical technique is that the surface microstructure can be controlled relatively easily and accurately by changing the deposition conditions such as electrolyte, precipitation potential, and so on. Progress has been made in developing cost-effective and simple methods for growing more controlled nanostructures as well as creating more complex heterostructures. Although several successful strategies (oxidation, wet-chemical methods based on lead templates, and physical techniques such as sputtering and pulsed laser deposition) have been reported, electrochemical methods are a high-throughput method for synthesizing transition metal oxide nanostructure arrays with precise structure control. Therefore, in order to create higher performance LIBs, it is necessary to develop new methods in which both the particle size can be easily controlled, and the interface defects can be

reduced. In this context, electrochemical methods are seen as promising methods because they have parameters that will allow the formation of environmentally friendly, practical, inexpensive, size-controlled, and low-defect interfaces.[13] Since the thickness of the deposit can be easily controlled by adjusting the deposition time, and it is suitable for deposition at a single potential from the same environment, this method has been used very successfully by other scientists in coating very complex systems such as nanotubes and nanowires with semiconductor materials.[4,5]

High-performance transition metal oxide for LIBs applications, a Co_3O_4 layer was directly prepared on the electrochemically synthesized NiO in a single step and simultaneously, at room temperature and atmospheric pressure, economically, without the need for additional steps and further processing as an electrochemical method for direct growth of electrode materials without binders. The excellent metal oxides used to improve the properties of LIBs, which are defined as the technology of the future, increase the active surface area and maximize the power density by reducing the internal resistance. During the electrochemical synthesis of NiO-Co_3O_4 nanostructures with the desired composition, structure, and size with an electrochemical method, the electrochemical deposition parameters such as deposition time, potential, current density, and electrolyte composition were changed, and NiO and Co_3O_4 in optimum size and structure were synthesized and characterized in a controlled manner.

EXPERIMENTAL

Materials

Chemical, Reagents and Analytical Conditions

A BAS 100B/W electrochemical workstation connected to a three-electrode cell (C3 Cell Stand, BAS) was used for the electrochemical experiments. The powder X-ray diffractograms of the deposited films were recorded using a Rigaku powder X-ray diffractometer with a CuKalpha radiation source (λ = 1.5406 Å). The morphological investigation and the elemental composition determination of metal oxide nanostructures were carried out by scanning electron microscopy (SEM) and energy dispersive X-ray analysis, respectively. Morphological work out and identify of the elemental composition (Ni/O), and (Co/O) of NiO-Co_2O_3 nanostructures were performed by an energy dispersive X-ray spectroscopy (EDS) united with a scanning electron microscope (ZEISS system).

Absorption measurements were performed using a Shimadzu UV-3101 UV-vis spectrometer at room temperature. In all cases, a Ag/AgCl (3 M NaCl) electrode served as the reference electrode, and a platinum wire was used as the counter electrode. A polycrystalline Au electrode (99.99% pure) was used as the working electrode for the electrochemical measurements, while ITO-coated quartz (10 cm^{-2}) was used for the UV-vis measurements. All of the electrolyte solutions used in this study were prepared using deionized water (*i.e.*, >18 M) from a Milli-system and were deoxygenated by purging the solution with N_2 for 10 min before performing the oxygen-free experiments.

In this study, high-performance NiO-Co_3O_4 electrode materials were synthesized electrochemically and these electrodes were formed by reduction at certain potentials in a solution medium saturated with O_2 and containing Ni^{2+} and Co^{2+} cations, and their surface properties were directly characterized (Figure 1). It is thought that the NiO and Co_3O_4 nanostructures formed on the ITO substrate will increase the efficiency by providing features such as increased surface area, better capacitance and conversion stability. Electrochemically formed ITO/NiO/Co_3O_4 nanostructured electrodes were formed for the first time by depositing an electrochemical method developed by us. With this method, both the interface defects of ITO/NiO/Co_3O_4 electrodes will be eliminated and size-controlled nanostructures will be synthesized. Since the ITO/NiO/Co_3O_4 nanostructured electrodes, which are thought can be used in LIBs, are more active for binary metal oxide redox, they are electrochemically designed to form this electrode with the most suitable structure, morphology, size and composition. By systematically changing the electrochemical parameters, electrolyte type and composition, good conductivity can be created resulting in excellent energy power density.

RESULTS AND DISCUSSION

Optimum electrochemical deposition parameters and deposition potentials obtained from these voltammetric studies were determined. At potentials more than 900 mV, bulk deposition of Co_3O_4 occurs. All these electrochemical observations show that a Co monolayer was formed on the Au electrode surface and then oxidized, and as a result, the Au electrode surface was coated with the Co_3O_4 compound. As seen in the voltammogram in Figure 2A first observed at 288 mV; attributed to the redox of CoOOH/Co_3O_4 ($Co_3O_4+OH^- \leftrightarrow CoOOH+e^-$) and the CoO_2/CoOOH pair appearing at the second 342 mV; ($CoOOH+OH^- \leftrightarrow CoO_2+H_2O+e^-$). Firstly, synthesis of Co_3O_4 nanostructures[14] from a solution containing aqueous 2mM $Co(NO_3)_2$ (as Co^{+2} source), 0.5 M $KHCO_3$ suspension, and dissolved O_2 gas was carried out using electrochemical deposition technique. Since the solubility of the dispersed aqueous suspension of Co_3O_4 depends on pH, temperature, particle size, and ionic strength, the amount of dissolved Co^{2+} can be adjusted by controlling these parameters. Before performing the electrochemical deposition, cyclic voltammo-

grams for Co were taken from the solution saturated with O_2, and the approximate deposition potential (900 mV) for deposition was determined. With the electrochemical process, well-arranged Co_3O_4 films were formed and characterized by electrodeposition at a single potential suitable for the potential of Co_3O_4. If the electrode potential is kept constant at the bulk potential of Co in the presence of dissolved O_2 and aqueous Co_3O_4 suspension, metallic Co monolayers and then Co oxidized to Co_3O_4 and Co_3O_4 was grown on the Au electrode at 900 mV, which is the electrochemically optimal potential.

The voltammograms of the Au(111) working electrode taken at room temperature in an O_2 saturated solution containing 2 mM $NiSO_4$ - 0.1 M Na_2SO_4 and 0.1 M acetate buffer (pH:4.66) are given in Figure 2b. When converting from the conversion potential (-900 mV) by scanning the potential of the gold working electrode from 500 mV towards the cathodic potentials, the C1 peak (-134 mV) alternating with the A1 peak (-50 mV) corresponds to the sub-potential of nickel on the Au(111) electrode, and the C2 peak (-440 mV) corresponds to the bulk deposition of nickel. In the environment where the solution pH is 4.66, the sub potential deposition of nickel on the Au(111) electrode starts at -134 mV, and bulk deposition occurs at more negative potentials than -440 mV (Figure 2B). As a result, considering the voltammograms of the deposition potential regions of nickel in 0.1 M acetate buffer (pH=4.66) solution (0.1 M Na_2SO_4) on the Au(111) single crystal electrode at room temperature, If the potential of the gold working electrode is kept constant at -650 mV, NiO electrodeposition will occur. In the subsequent NiO characterization processes, electrochemical synthesis processes were carried out by keeping the potential constant at -650 mV. When the electrodeposition time reached 10 minutes, it was observed that the average size of the NiO nanoparticles, which grew on the substrate and started to become clear, increased and reached dimensions of 200 nm. In short, as can be seen from Figure 2B, the size of the crystals increase with the deposition time. Co_3O_4 crystal structures were deposited on NiO synthesized in the most suitable parameters optimized for both metal oxides and their characterization was carried out.

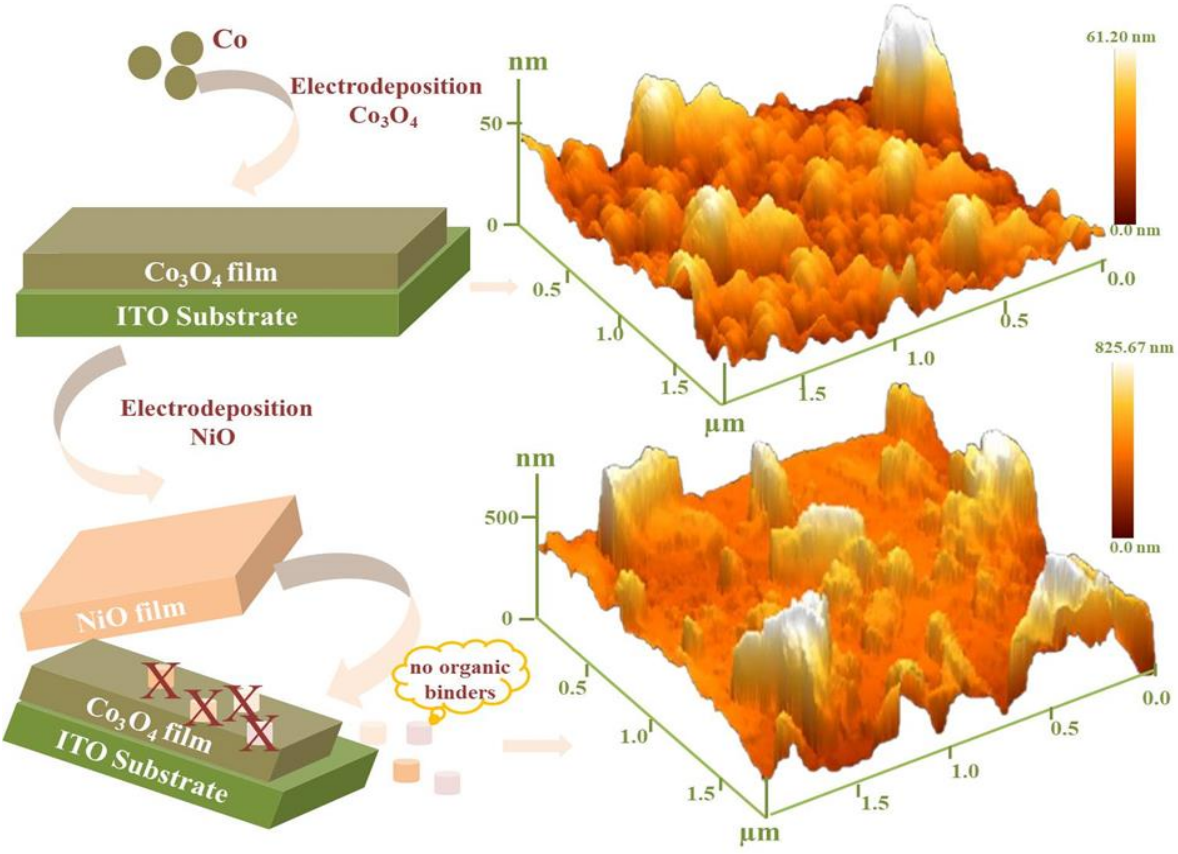

Fig. 1 – Schematic representation of the synthesis of NiO/Co_3O_4 nanostructured arrays on ITO.

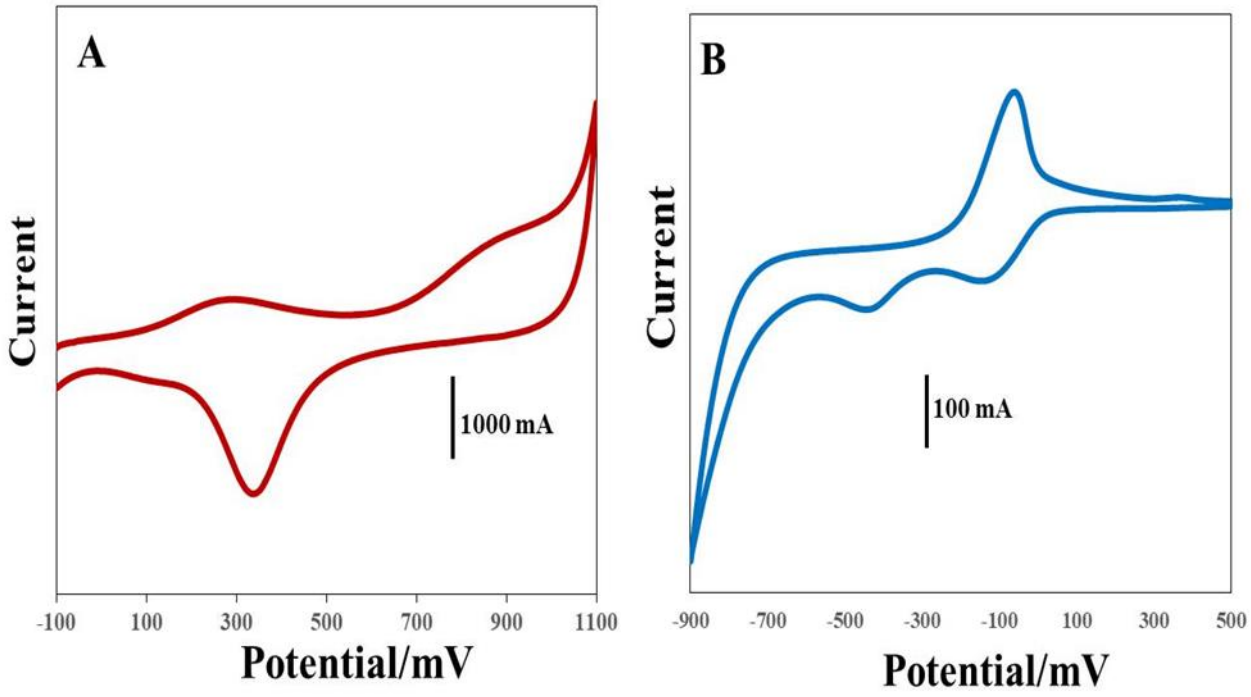

Fig. 2 – Cyclic voltammograms of the Au(111) substrate recorded at 100 mV/s in solution saturated with O_2 gas containing: (A) 2mM $Co(NO_3)_2$ and 0.5 M $KHCO_3$, (B) 2 mM $NiSO_4$ and 0.1 M Na_2SO_4 (pH: 4.66).

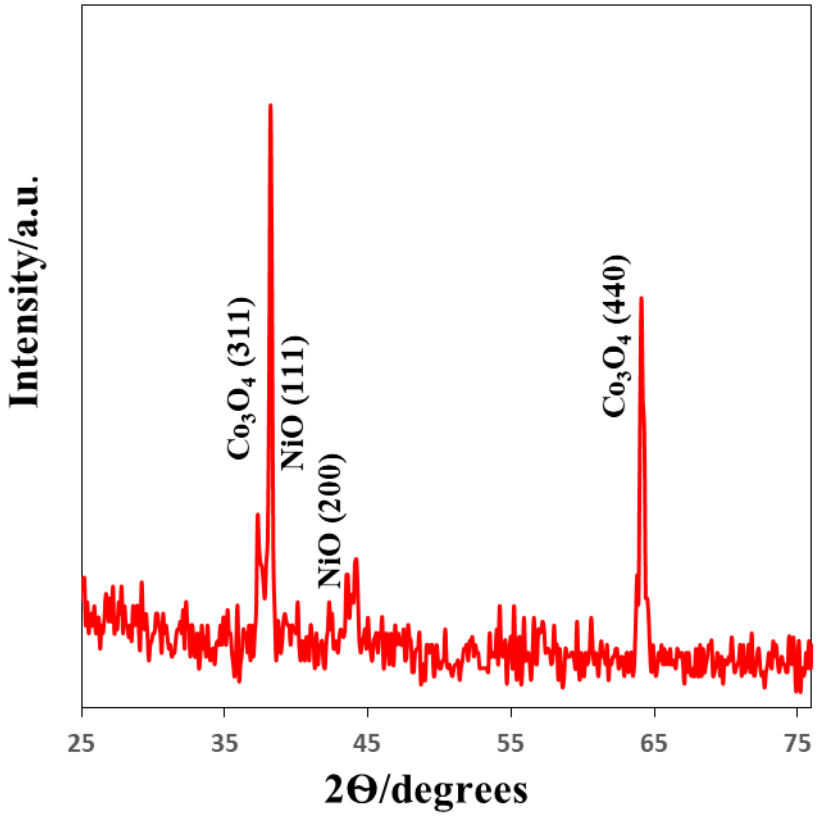

Fig. 3 – XRD patterns of the deposited films of NiO/Co_3O_4 (10 min at 900 mV, 10 min Co_3O_4 on NiO - 650 mV for 5 min).

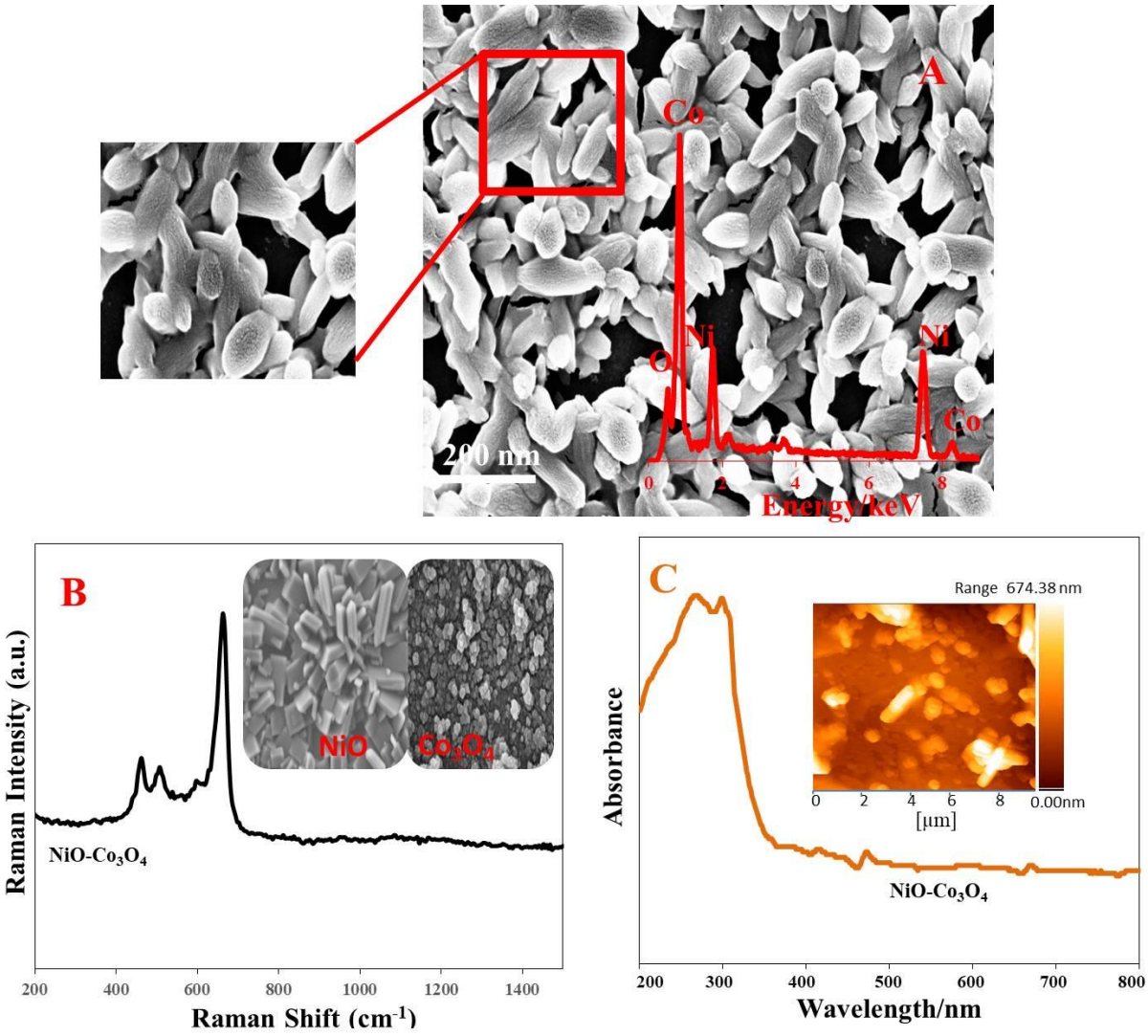

Fig. 4 – SEM, EDS images of films obtained by the deposition of (A) (-650 mV) 10 minutes NiO -(900 mV) 5 minutes Co_3O_4, (B) Micro-Raman spectra of deposition) films measured by planar oriented laser polarization NiO on ITO-coated glass electrode at room temperature (10 min deposition at -650 mV), NiO/ Co_3O_4 (10 min deposition at 900 mV on Co_3O_4) on ITO-coated glass electrode and (C) UV-visible absorption spectra of NiO/ Co_3O_4 (10 min deposition at 900 mV on Co_3O_4) on ITO-coated glass electrode.

Electrochemically synthesized NiO/Co_3O_4 nanostructured electrodes with potential controlled deposition by electrochemical method were economically prepared directly on ITO and Au(111) at room temperature and atmospheric pressure, without the need for additional steps and further processing. In addition, with this method, NiO/Co_3O_4 on ITO and Au(111), which have the desired composition, structure and size, were easily synthesized by controlling electrochemical parameters such as potential and time. Here, as in NiO, the fact that Co_3O_4 reaches its bulk values at approximately the same time is due to the similarity of deposition kinetics and lattice constants, and thus homogeneous films with high crystalline structure are formed.

Figure 3 is the XRD diffractograms of two compound metal oxide (NiO-Co_3O_4) semiconductor films prepared in an aqueous medium. In order to better understand the cubic nanocrystal structures obtained from SEM and AFM studies, the crystallographic properties of NiO films were elucidated by X-ray diffraction. X-ray diffraction spectra of NiO films grown at a constant potential (-650 mV) in a solution containing 2 mM $NiSO_4$ saturated with O_2 and 0.1 M Na_2SO_4 (pH: 4.66) depending on time (30 minutes) are shown in Figure 3. This spectrum includes strong diffraction peaks at 2θ=37.28 and 43.25 originating from the (111) and (200) planes of NiO. The observation of very intense peaks belonging to the nanorod NiO phase indicates that NiO has a preferential

electrochemical growth orientation along the c-axis (lattice constants a = 8.3532 Å and c = 8.3532 Å, JCPDS card no. 01- 089-5881).[14,15]

The crystallographic properties of Co_3O_4 thin films grown by potential controlled electrolysis method in an oxygen-saturated aqueous solution of Co at 900 mV for 5 minutes were determined by XRD (X-ray diffraction) spectra. In the XRD diffractogram of the electrodeposited Co_3O_4 given in Figure 3, Co_3O_4 (311) at 2θ=36.9, Co_3O_4 (440) at 2θ=65.3, the XRD diffraction peak is clearly seen. The observation of very intense peaks belonging to the nanodisk Co_3O_4 phase indicates that Co_3O_4 has a preferential electrochemical growth orientation along the c-axis (lattice constants a = 8.1980 Å and c = 8.1980 Å, JCPDS card no. 98-006-9373). Again, the absence of any peak in the XRD patterns of other impurities such as cobalt hydroxide and metallic cobalt can be considered as the biggest evidence of pure Co_3O_4 formation.[16] At the same time, the fact that this XRD diffractogram does not contain any peaks originating from other phases such as Ni, nickel hydroxide, Co and kobalt hydroxide other than NiO, Co_3O_4 can be accepted as proof of the high purity of cubic NiO and Co_3O_4 crystals grown from the same solution by a deposition method.

SEM images of electrochemically obtained NiO-Co_3O_4 films, 10 min NiO (900 mV) 5 min Co_3O_4 (-650 mV) deposition from a solution saturated with O_2 on ITO substrate at room temperature by potential controlled electrolysis method is shown in Figure 4A. It is clearly seen that homogeneous nanobelt-like structures in the SEM image of the films are obtained in the structures formed by modifying Co_3O_4 for 60 minutes at 900 mV on NiO for 10 minutes at -650 mV (Figure 4A). As can be seen from the SEM images, by changing the deposition times of Co_3O_4 on NiO metal oxides, materials with desired properties can be easily formed without using any organic binders.

The qualitative and quantitative determination of the components on the surface of the examined sample and the presence of elements other than the desired in the sample can be determined by the EDS technique. EDS is often combined with SEM. This technique, which has a high characterization ability, also gives the ratio of elements in the existing NiO-Co_3O_4. The EDS spectrum given in Figure 4A shows that, as in the XRD patterns, the elemental composition (Co/O/Ni) of Co_3O_4/NiO films was determined using the EDS technique. EDS analysis of NiO-Co_3O_4 films deposited on ITO substrates is given in Figure 4B. Qualitative analyzes of the EDS spectra of films containing cobalt, oxygen, and nickel show that (0.5/2/1) Co, O, and Ni are present for films with Co_3O_4 modification on NiO films in the structure. By changing the deposition time and adjusting the composition ratio, the desired stoichiometry can be achieved in the films.

Figure 4B shows Raman spectra measured by planar oriented laser polarization of deposition of NiO/Co_3O_4 on ITO electrode (Co_3O_4 5 minutes at -650 mV on 10 minutes at 900 mV 10 minutes NiO) films. In the Raman spectrum of the NiO/Co_3O_4 sample, different bands are observed in Figure 4B. In the Raman spectra of NiO nanocrystals with grain sizes of 300 nm and 100 nm, the peaks originating from single-phonon (1P), two-phonon (2P) scattering is indicated by the vibration source of the first four bands → one phonon (1P) TO / LO, two phonons (2P) 2TO, TO + LO and 2LO modes (Figure 4B). The band transverse optical (TO) and 614 cm^{-1} longitudinal optical (LO) phonon, observed at 457 cm^{-1} using the 532 nm excitation wavelength in the spectrum of NiO at room temperature in micro-raman, represent the modes of NiO single crystals and the 632 cm^{-1} longitudinal optical (LO) phonon, if 2TO, 935 cm^{-1} TO+LO, 991 cm^{-1} 2LO NiO modes correspond to combination phonon modes. The bands of these prominent Raman spectra of 476 cm^{-1}, 520cm^{-1}, and 676 cm^{-1} correspond to the modes of the Co_3O_4 particle phase.

Molecular absorption studies were carried out to explain the quantum confinement effects of NiO/ Co_3O_4 nanoparticles (Figure 4C). Molecular absorption spectra of NiO/Co_3O_4 nanoparticles formed at different film thicknesses on ITO (indium tin oxide) coated glass electrodes are given in Figure 4C. The wavelength values at which the absorption of NiO/Co_3O_4 particles begin, and thus the change in energy values are shown. It was observed that as the amount of Co in the NiO films decreased, the energy and wavenumber of the films increased, and the absorption wavelengths shifted to blue (Figure 4C). Therefore, NiO/Co_3O_4 films with the desired energy properties in the region within the bandgap energy were prepared by changing the film thickness (NiO and Co_3O_4) by deposition at different times in NiO and Co_3O_4 semiconductors.

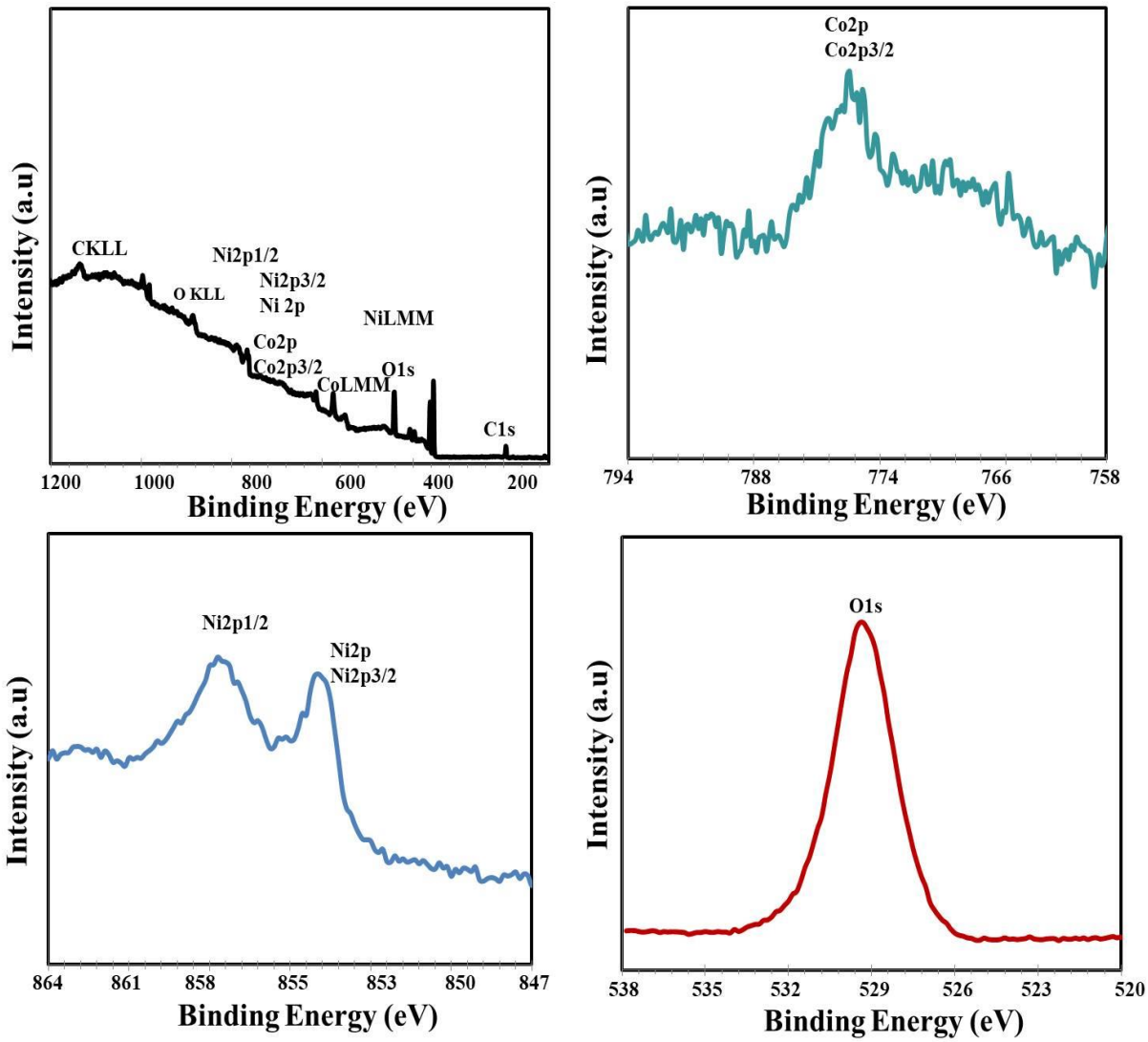

Fig. 5 – XPS spectra of Co 2p and Ni 2p and O 1s of NiO/ Co_3O_4 deposited on the ITO electrode.

As a result, SEM and AFM images of NiO-Co_3O_4 films, which were deposited at different times, support each other. AFM studies were carried out in order to examine the NiO/Co_3O_4 structures formed with the increasing film thickness with the increase of the deposition time. The AFM images in Figure 4C show that the crystal size of the films increases with increasing deposition time. Growth in all three directions with increasing deposition time is an indication of a 3-dimensional nucleation and growth kinetics. Figure 4C is an AFM image of the surface morphology of NiO/Co_3O_4 deposited on the substrate surface after deposition with a potential controlled electrolysis method is observed that nanoparticles, whose thickness, width, and number increase with increasing deposition time, deposit on the gold surface homogeneously

X-ray photoelectron spectroscopy, used for the qualitative and quantitative characterization of ITO-Co_3O_4 and ITO-NiO nanostructured films, was used to determine whether Co_3O_4 and NiO are in the desired elemental composition and to determine the oxidation steps of Co[18] and Ni.[19] This technique is based on the removal of electrons from the inner shell as a result of exposure of the electrode surfaces with X-rays and the measurement of the kinetic energies of these removed electrons. The measured kinetic energies of photoelectrons carry information about both the elemental composition of the surface and the oxidation stages of these elements. XPS analyzes were carried out in order to get more detailed information about the type of surface components in NiO-Co_3O_4 films (Figure 5), which were partially analyzed qualitatively by EDS technique,

and also to determine the oxidation steps of these components. Using a fitting method, it can be placed within a broad spectrum. The XPS profile for the Co 2p region (Figure 5) shows two peaks at 780.1 eV and 795.4 eV, which contribute to Co2p3/2 and Co2p 1/2, respectively. Moreover, the partition width between Co2p 3/2 and Co2p1/2 is about 15.3 eV corresponding to Co_3O_4. As shown in Figure 5, the binding energies of the main peaks at 855.7 eV and 873.5 eV correspond to the Ni2p3/2 edge and Ni2p1/2 in the Ni2p region (Figure 5), respectively. All data in the spectra shown in Figure 5 are calibrated against the C1s standard peak at 284.6 eV. Since the positions of the binding energies of the Co 2p peaks in the synthesized samples (783.4 eV and 812.6 eV for Co 2p3/2 and Co 2p1/2, respectively) match exactly with the standard data of cobalt oxide, it is thought that Co in the films has +4 oxidation.[20] It is clearly seen in Figure 5 that the peak in the XPS spectrum obtained for O1s is sharp and symmetrical. It has been reported in the literature studies on this subject that the nature of this peak, centered at 530.8 eV, observed for Co_3O_4 thin films corresponds to various bindings of oxygen in the films. It has been shown that this broad O 1s peak is actually the result of an XPS peak with binding energies of 530.7 eV.

The separation of the main binding energy peaks is 17.5 eV, indicating the presence of NiO in the samples. In addition, two peaks can be observed at the Ni 2p 3/2 edge and at the Ni 2p 1/2 on the high binding energy side. It shows the O1s region (Figure 5) from the samples, and the 531.4 eV band contributing to M-O (M: Ni-Co) indicates the presence of lattice oxygen in the prepared samples. The XPS results show that the Ni-Co oxide is a suitable mixture of Co_3O_4 and NiO in the XRD arrangement. All data in the spectra shown in Figure 5 are calibrated against the C1s standard peak at 284.6 eV. Since the positions of the binding energies of the Ni 2p peaks in the synthesized samples (855.4 eV and 876.6 eV for Ni 2p3/2 and Ni 2p1/2, respectively) exactly match the standard data of zinc oxide, it is thought that Ni in the films has +2 oxidation state O1s. It can be clearly seen from Figure 5c that the peak in the XPS spectrum obtained for XPS is broad and asymmetrical. This broad O 1s peak has been shown to be actually the resultant of two XPS peaks with binding energies of 529.7 eV and 530.7 eV; the first O 1s peak was was thought to be due to the most intense peak in NiO thin films, which is known to originate from O^{2-} ions surrounded by Ni atoms in the wurtzite structure; The second peak was thought to be due to the presence of weakly bound oxygen species or hydroxyl groups on the film surface.

CONCLUSIONS

Nanostructures of transition metal oxides such as NiO and Co_3O_4 are formed by combining three-dimensional and ordered nanostructures. Thanks to the developed electrochemical method, the synthesis of these metal oxides on ITO substrates was done in a practical and inexpensive way. In the electrochemical synthesis of NiO-Co_3O_4 nanostructures, by changing the electrochemical deposition parameters such as deposition time, potential, current density and electrolyte composition, these transition metal oxides were obtained in optimal size and structure and their characterization was carried out. Thus, the synthesis of NiO-Co_3O_4 with high conversion efficiency, with parameters that allow interface and size-controlled material deposition, was achieved by electrochemical methods, and this process was accomplished without using any organic binders between these binary metal oxide structures. NiO/Co_3O_4 electrodes, which are economically prepared at room temperature and atmospheric pressure without the need for additional steps and further processing, are promising materials for LIBs applications.

Acknowledgements. The author disclosed receipt of the following financial support for the research, authorship, and publication of this article: We are grateful to Ataturk University BAP (Project No. FD-6610) for their financial support.

REFERENCES

1. F. Cheng, Z. Tao, J. Liang and J. Chen, *Chem. Mater.*, **2008**, *20*, 667-681.
2. T. Zhang, D. Li, Z. Tao and J. Chen, *Progress in Natural Sci.: Mater. Int.*, **2013**, *23*, 256-272
3. K. T. Nam, D. W. Kim, P. J. Yoo, C. Y. Chiang, N. Meethong, P. T.Hammond, Y. M. Chiang and A. M. Belcher, *Science*, **2006**, *312*, 885-890.
4. C. Gu, H. Xu, M. Park and C. Shannon, *Langmuir*, **2009**, *25*, 410-414.
5. W. Zhu, X. Liu, H. Liu, D. Tong, J. Yang and J. Peng, *J. Am. Chem. Soc.*, **2010**, *132*, 12619-12626.
6. X. W. Wang, D. L. Zheng, P. Z. Yang, X. E. Wang, Q. Q. Zhu, P. F. Ma and L.Y. Sun, *Chem. Phys. Lett.*, **2017**, *667*, 260-266.

7. N. Zhao, H. Fan, M. Zhang, J. Ma, Z. Du, B. Yan, H. Li and X. Jiang, *Chem. Engineer. J.*, **2020,** *390*, 124477-124482.
8. X. Wang, L. Sunc, X. Suna, X. Lid and D. Hea, *Mater. Research Bull.*, **2017**, *96*, 533-537.
9. G. K. Veerasubramani, K. Krishnamoorthy and S. J. Kim, *J. Power Sources*, **2016**, *306*, 378–386.
10. T. N. Ly and S. Park, *J. Ind. Engineer. Chem.*, **2018**, *67*, 417-428.
11. Z. Zeng, B. Xiao, X. Zhu, J. Zhu, D. Xiao and J. Zhu, *Ceramics Int.*, **2017**, *43*, S633-S638.
12. B. Guo, C. Li and Z. Yuan, *J. Phys. Chem. C*, **2010**, *114*, 12805–12817.
13. B. W. Gregory and J. L. X. Stickney, *J. Electroanal. Chem.*, **1991**, *300*, 543-548.
14. P. Jiang, Q. Wang, J. Dai, W. Li and Z. Wei, Mater. Lett., 2017, 188, 69-72.
15. B. Varghese, M. V. Reddy, Z. Yanwu, C. Sheh Lit, T. C. Hoong, G. V. Subba Rao, B. V. R. Chowdari, A. T. S. Wee, C. T. Lim and C. Sow, Chem. Mater., 2008, 20, 3360–3367.
16. B. Guo, C. Li and Z. Yuan, J. Phys. Chem. C, 2010, 114, 12805–12817.
17. S. G. Kandalkar, H. Lee, H. Chae and C. Kim, *Mater. Research Bull.*, **2011**, *46*, 48-51.
18. X. Xia, J. Tu, Y. Zhang, X. Wang, C. Gu, X. Zhao and H. J. Fan, *ACS nano*, **2012**, *6*, 5531–5538.
19. R. Patel, A. I. Inamdar, B. Hou, S. Cha, A. T. Ansari, J. L. Gunjakar, H. Im and H. Kim, *Curr. Appl. Phys.*, **2017**, *17*, 501-506.
20. C. Elmı, S. Gugggenheım and R. Gıeré, *Clays and Clay Minerals*, **2016**, *64*, 537–551.